
JEJU NATIONAL UNIVERSITY 1952
JEJU
1952
제주대학교

Master's Thesis

The flavonoid luteolin inhibits cellular damage against oxidative stress via the induction of antioxidant defense system

Dong-Ok Ko

Department of Medicine

Graduate School

Jeju National University

February, 2010

산화적 스트레스로 유도된 세포손상에 대하여 항산화효소 활성을 통한 flavonoid 계열인 Luteolin 의 보호효과

지도교수 현진원

고동옥

이 논문을 의학 석사학위 논문으로 제출함

2010 년 2 월

고동옥의 의학 석사학위 논문을 인준함

심사위원장 姜奈昊 印

위 원 高榮祥 印

위 원 玄鎭姸 印

제주대학교 대학원

2010 년 2 월

The flavonoid luteolin inhibits cellular damage against oxidative stress via the induction of antioxidant defense system

Dong-Ok Ko

(Supervised by Professor **Jin-Won Hyun**)

A thesis submitted in partial fulfillment of the requirement for degree of

Master of Science in Medicine

2010. 2.

This thesis has been examined and approved

Dec 29, 2009

Department of Medicine

Graduate School

Jeju National University

February, 2010

Abstract

The present stuty was to investigate the cytoprotective effects of luteolin against the oxidative stress induced by hydrogen peroxide (H_2O_2). We found that luteolin scvanged superoxide and hydroxyl radicals generated by xanthine/xanthine oxidase and Fenton reaction ($FeSO_4/H_2O_2$), respectively, in a cell-free chemical system. In addition, a marked increase in cellular reactive oxygen species (ROS) was observed in H_2O_2-induced Chinese hamster lung fibroblasts (V79-4) cells. Luteolin significantly decreased the level of H_2O_2-induced intracellular ROS and damage to cellular components such as the lipid, DNA. Luteolin enhanced cell viability that decreased after H_2O_2 treatment and reduced H_2O_2-induced apoptosis via inhibition of mitochondria mediated caspases pathway. Luteolin reduced the levels of the active forms of caspase 9 and 3, reduced the expression of Bax and elevated the expression of bcl-2. Furthermore, luteolin restored the level of reduced glutathione (GSH) by H_2O_2 treatment and protein expression of a catalytically active subunit of glutamate-cysteine ligase (GCL), which is a rate-limiting enzyme in GSH biosynthesis. In addition to, luteolin increased the activities and the protein expression of cellular antioxidant enzymes like, superoxide dismutase (SOD), catalase (CAT), glutathione peroxidase (GPx) and hemeoxygenase-1 (HO-1). Our data suggested that luteolin prevents the cellular damage against hydrogen peroxide by inhibition of ROS and induction of antioxidant enzymes.

Key word: luteolin; reactive oxygen species; lipid peroxidation; DNA damage; antioxidant enzymes.

CONTENTS

LIST OF FIGURES

1. Introduction

Reactive oxygen species (ROS) are free radicals such as superoxide anion (O_2^-), hydroxyl radical (OH^-) and hydrogen peroxide (H_2O_2). ROS is formed as a natural byproduct of the normal metabolism of oxygen and have important roles in immume response and cell proliferation [1-2]. In the other hands, environmental stress such as UV and ionizing radiation can significantly increase the ROS level and damage to the cell [3-4]. Overproduction of ROS causes many diseases incuding cancer, lung toxicity and asthma [5-7]. For the protection against ROS, the cells have a variety of antioxidant enzymes such as superoxide dismutases (SOD), catalase (CAT), glutathione (GSH) and glutathione peroxidase (Gpx). Superoxide dismutases can catalyze the of superoxide anion into hydrogen peroxide (H_2O_2) and water. Catalase decomposites the H_2O_2 into oxygen and water, glutathione peroxidase destroys toxic peroxides. Hemeoxygenase-1 (HO-1) is also a defensive enzyme against oxidative stress. HO-1 degrades heme into carbon monoxide (CO), iron, and biliverdin. It is strongly induced by the oxidative stress and protects jurkat T cell and microglial cell [8-9]. Flavonoids are abundantly found in fruits and vegetables. Flavonoids have been reported to exert ROS scavenging effects and antitumor effects [10-11].

Luteolin (3′,4′,5,7-tetrahydroxyflavone), a member of the flavonoid family, is isolated from celery, green peppers, perilla leaf, and camomile tea [12]. Moreover, luteolin has antitumor effect in a variety of cancer cells such as colorectal cancer, HCT116 colon cells and cervical cancer HeLa cells [13-14]. Furthermore, luteolin has protective effect against the toxicity in vivo [15-16]. Moreover, luteolin has anti-inflammtary properties [17]. Many reserchers have studied the effect of luteolin in a variety of cells. However, antioxident effect of luteolin in lung cells has not been reported until now. The present study to investigate the cytoprotective effect of luteolin via the antioxidant enzyme activation.

2. Materials and methods

2.1 Reagents

Luteolin (3′,4′,5,7-tetrahydroxyflavone, Fig.1) compound, 5,5-dimethyl-1-pyrroline-N-oxide (DMPO), Xanthine, Xanthine oxidase, 2′,7′-dichlorodihydrofluorescein diacetate(DCF-DA), Hoechst 33342 and Propidium iodide (PI) were purchased from Sigma Chemical company. (St.Louis, Mo) DPPP (Diphenyl-1-pyrenylphosphine) was purchased from molecular probe company (USA) and thiobarbituric acid from BDH Laboratories. (Poole, Dorset, UK) The primary anti-phospho histone H2A.X antibody was purchased from Upstate Biotechnology (Lake Placid, NY, USA) and the primary anti-Bax, Bcl-2, Gpx from Santa Cruz Biotechnology Inc.(Santa Cruz, CA, USA) and the primary caspase-3, 9 from Cell Signaling Technology (MA, USA) and the primary γ-GCL and HO-1 from Stressgen Company (Victoria, Canada) and the primary SOD, Catalase from Biodesign International Company (Maine, USA).

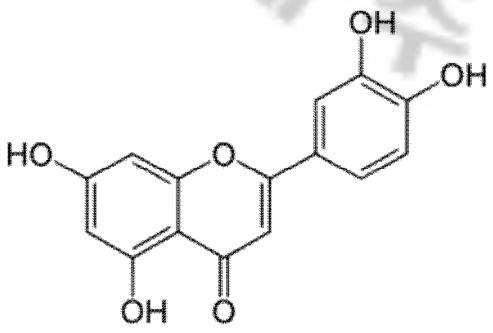

FIG 1. Chemical structure of luteolin

2.2. Cell culture

To study the effect of luteolin on oxidative stress, the chinese hamster lung fibroblast cells (V79-4) were used. The cells were maintained at 37 °C in an incubator, with a Humidified atmosphere of 5% CO_2, and cultured in Dulbecco's modified Eagle's medium containing 10% heat-inactivated fetal calf serum, streptomycin (100µg/ml) and penicillin (100 U/ml).

2.3. Detection of hydroxyl radical

Hydroxyl radicals were generated by the Fenton reaction (H_2O_2+$FeSO_4$), which were then quickly reacted with a nitrone spin trap, 5,5-dimethyl-1-pyrroline-N-oxide (DMPO). The resultant DMPO-OH adducts were detected using an ESR spectrometer. The ESR spectrum was recorded using JES-FA ESR spectrometer (JEOL, Tokyo, Japan), at 2.5 min after being mixed in a phosphate buffer solution (pH 7.4) with 0.2 ml of 0.3 M DMPO, 0.2 ml of 10 mM $FeSO_4$, 0.2 ml of 10 mM H_2O_2, and 2.5µg/ml luteolin. The parameters of the ESR spectrometer were set at the following conditions: magnetic field of 336.5 mT, power of 1.00 mW, frequency of 9.4380 GHz, modulation amplitude of 0.2 mT, gain of 200, scan time of 0.5 min, scan width of 10 mT, time constant of 0.03 s, and a temperature of 25 °C [18-19].

2.4. Detection of superoxide anion

Superoxide anions were generated by Xanthine+xanthine oxidase which were then quickly reacted with a nitrone spin trap, 5,5-dimethyl-1-pyrroline-N-oxide (DMPO). The resultant DMPO-OH adducts were detected using an ESR spectrometer. The ESR spectrum was recorded using JES-FA ESR spectrometer (JEOL, Tokyo, Japan), at 2.5 min after being mixed in a phosphate buffer solution (pH 7.4) with 0.2 ml of 6M DMPO, 0.2ml of 10mM Xanthine,0.2ml of 0.5U xanthine oxidase and 2.5 µg/ml luteolin. The parameters of the ESR spectrometer were set at the following conditions: magnetic field of 336.5 mT, power of 1.00 mW, frequency of 9.4380 GHz, modulation amplitude of 0.2 mT, gain of 200, scan time of 0.5 min, scan width of 10 mT, time constant of 0.03 s, and a temperature of 25 °C [18-19].

2.5. Intracellular reactive oxygen species (ROS) measurement

The DCF-DA method was used to detect the levels of intracellular ROS [20]. The image analysis for the generation of intracellular ROS was achieved by seeding the cells on a cover-slip loaded six well plate at 1.5×10^5 cells/well. Sixteen hours after plating, the cells were treated with luteolin at 2.5µg/ml. After 30 min, 1mM of H_2O_2 was added to the plate. After changing the media, 100 µM of DCF-DA was added to each well and was incubated for an additional 30

min at 37 °C. After washing with PBS, the stained cells were mounted onto microscope slide in mounting medium (DAKO, Carpinteria, CA, USA). Microscopic images were collected using the Laser Scanning Microscope 5 PASCAL program (Carl Zeiss, Jena, Germany) on a confocal microscope.

2.6. Lipid peroxidation assay

Lipid peroxidation was estimated by using a DPPP fluorescent probe as described by Okimoto et al [21]. After V79-4 cells (1×10^5cell/ml) were incubated with 5 μM DPPP for 15 min in the dark, the images of DPPP fluorescence by reactive species were analyzed by the Zeiss Axiovert 200 inverted microscope at fluorescence in the DAPI region (excitation, 351 nm; emission, 380 nm). Lipid peroxidation was also assayed by the thiobarbituric acid reaction [22]. The cells were thenwashed with cold PBS, scraped, and homogenized in ice-cold 1.15% KCl. One hundred μl of the cell lysates was mixed with 0.2ml of 8.1% sodium dodecylsulfate, 1.5ml of 20% acetic acid (adjusted to pH 3.5) and 1.5 ml of 0.8% thiobarbituric acid (TBA). The mixture was made up to a final volume of 4 ml with distilledwater and heated to 95 °C for 2 h. After cooling to room temperature, 5ml of n-butanol and pyridine mixture (15:1, v/v) was added to each sample and shaken. After centrifugation at 1000 ×g for 10 min, the supernatant fraction was isolated,

and the absorbance was measured spectrophotometrically at 532 nm. The amount of thiobarbituric acid reactive substance (TBARS) was determined using standard curve with 1,1, 3, 3-tetrahydroxypropane.

2.7. Comet assay

Cells were treated with luteolin at 2.5μg/ml for 30 min later, 1mM H_2O_2 was added and incubated for 15 min. The mixture was centrifuged at 13,000 ×g for 5 min and the cell pellet (0.5×10^5 cells) was mixed with 100 μl of 0.5% low melting agarose (LMA) at 39 °C and spread on a fully frosted microscopic slide that was pre-coated with 200 μl of 1% normal melting agarose (NMA). After solidification of the agarose, the slide was covered with another 75 μl of 0.5% LMA and then immersed in lysis solution (2.5 MNaCl, 100mM Na-EDTA, 10mMTris, 1% Trion X-100 and 10% DMSO, pH 10) for 1 h at 4 °C. The slides were then placed in a gel-electrophoresis apparatus containing 300mMNaOHand 10mMNa-EDTA (pH 13) for 40min to allow DNA unwinding and the expression of the alkali labile damage. An electrical field was applied (300 mA, 25 V) for 20 min at 4 °C to draw negatively charged DNA toward an anode. After electrophoresis, the slides were washed three times for 5 min at 4 °C in a neutralizing buffer (0.4 M Tris, pH 7.5) and then stained with 75 μl of ethidium bromide (20μg/ml).

The slides were observed using a fluorescence microscope and image analysis (Komet, Andor Technology, Belfast, UK). The percentage of total fluorescence in the tail and the tail length of the 50 cells per slide were recorded.

2.8. Western blot analysis

The cells were harvested, washed twice with PBS, lysed on ice for 30 min in 100 µl of a lysis buffer [120 mM NaCl, 40mM Tris (pH 8), 0.1% NP 40] and then centrifuged at 13,000×g for 15 min. The supernatants were collected from the lysates and the protein concentrations were determined. Aliquots of the lysates (40 µg of protein) were boiled for 5 min and electrophoresed in 10% sodium dodecylsulfate-polyacrylamidegel. The blots in the gels were transferred onto nitrocellulose membranes (Bio-Rad, Hercules, CA, USA), which were then incubated with the primary antibodies. The membranes were further incubated with the secondary immunoglobulin-G-horseradish peroxidase conjugates(Pierce, Rockford, IL, USA). Protein bands were detected using an enhanced chemiluminescence Western blotting detection kit (Amersham, Little Chalfont, Buckinghamshire, UK), and then exposed onto X-ray film.

2.9. MTT assay

To determine the effect of luteolin on the cell viability in H_2O_2 treatment, the cells were treated

with luteolin for 1 h at 2.5μg/ml. Next, 1 mM of H_2O_2 was added to the plate, and the mixture was incubated for 24 h. Fifty μl of the [3-(4, 5-dimethylthiazol-2-yl)-2, 5-diphenyltetrazolium] bromide (MTT) stock solution (2 mg/ml) was then added into each well to attain a total reaction volume of 200μl. After incubating for 4 h, the plate was centrifuged at 800×g for 5 min and the supernatants were aspirated. The formazan crystals in each well were dissolved in 150μl of dimethylsulfoxide and read at 540nm on a scanning multi-well spectrophotometer [23].

2.10. Nuclear staining with Hoechst 33342

The cells were treated with luteolin at 5 μM. After 1 h, 1mM of H_2O_2 was added to the plate, and the mixture was incubated for 24 h. 1.5μl of Hoechst 33342 (stock 10 mg/ml), a DNA specific fluorescent dye, was added to each well and incubated for 10 min at 37°C. The stained cells were then observed under a fluorescent microscope, which was equipped with a CoolSNAP-Pro color digital camera, in order to examine the degree of nuclear condensation.

2.11. Flow cytometry analysis

The cells were treated with luteolin at 2.5 μg/ml. After 1 h, 1 mM of H_2O_2 was added to the plate, and the mixture was incubated for 24 h. Flow cytometry was performed to determine the

content of apoptotic sub G_1 hypo-diploid cells [24]. The cells were harvested, and fixed in 1ml of 70% ethanol for 30 min at 4°C. The cells were washed twice with phosphate buffered saline (PBS), and then incubated for 30 min under dark condition at 37°C in 1 ml of PBS containing 100 µg propidium iodide and 100 µg RNase A. The flow cytometric analysis was performed and the proportion of sub G_1 hypo-diploid cells was assessed by the histograms generated using the computer program, Cell Quest and Mod-Fit.

2.12. GSH level detection

The intracelluar GSH level was determined by using a GSH-sensitive fluorescence dye CMAC. V79-4 cells (1×10^5 cells/ml) were incubated with 5 µM CMAC cell tracker for 30 min. The images of CMAC cell tracker fluorescence by GSH were analyzed by the Zeiss Axiovert 200 inverted microscope at fluorescence in the 4,6-diamidino-2-phenylindole (DAPI) region (excitation, 351 nm; emission, 380 nm) [25].

2.13. Catalase activity

The cells were seeded at 1×10^5 cells/ml, and at 24 h after plating, the cells were treated with luteolin for 3 h. The harvested cells were suspended in 10 mM phosphate buffer (pH 7.5) and

then lysed on ice by sonication twice for 15 s. TritonX-100 (1%) was then added to the lysates which were further incubated for 10min on ice. The lysates were centrifuged at 5000×g for 30 min at 4◦C to remove the cellular debris and the protein content was determined. For detection catalase activity, 50µg of protein was added to 50 mM of phosphate buffer (pH 7) containing 100 mM (v/v) of H_2O_2. The reaction mixture was incubated for 2 min at 37◦C and the absorbance monitored at 240 nm for 5min. Changes in absorbance with time was proportional to the breakdown of H_2O_2.

2.14. Glutathione peroxidase (Gpx) activity

Fifty micrograms of the protein was added to 25 mM of the phosphate buffer (pH 7.5), 1 mM EDTA, 1 mM NaN3, 1 mM glutathione, 0.25 unit of glutathione reductase, and 0.1 mM NADPH. After incubation for 10 min at 37◦C, H_2O_2 was added to the reaction mixture at a final concentration of 1 mM. The absorbance was monitored at 340 nm for 5 min. The glutathione peroxidase activity was measured as the rate of NADPH oxidation at 340 nm [26]. The glutathione peroixdase activity is expressed as units/mg protein.

2.15. HO-1 activity assay

HO-1 enzyme activity was measured as described previously [27] Cells were homogenized in 0.5 ml ice-cold 0.25 M sucrose solution containing 50 mM potassium phosphate buffer (pH 7.4). Homogenates were centrifuged at 200 g for 10 min. The supernatants were centrifuged at 9000g for 20 min, and further centrifuged at 105,000 g for 60 min. The pellet was then resuspended in 50 mM potassium phosphate buffer (pH 7.4) and the amount of protein was determined by Bradford method [28]. The reaction mixture (200 µl) containing 0.2 mM of the substrate hemin, 500g/ml of cell lysate, 0.5 mg/ml rat liver cytosol as a source of biliveridin reductase, 0.2 mM $MgCl_2$, 2mM glucose-6-phosphate, 1 U/ml glucose-6-phosphate dehydrogenase, 1 mM NADPH and 50mM potassium phosphate buffer (pH 7.4) was incubated at 37◦C for 2 h. The reaction was stopped with 0.6 ml of chloroform and after extraction, the chloroform layer was measured spectrophotometrically. Bilirubin formation was calculated from the difference in absorption between 464 and 530 nm.

2.16. SOD activity assay

The V79-4 cells were seeded in a culture dish at a concentration of 1×10^5 cells/ml and, 24 h after plating, were treated with luteolin at 2.5 µg/ml. After 1 h, 1 mM H_2O_2 was added to the

plate, which was incubated more for a further 1 h. The cells were then washed with cold PBS and scraped. The harvested cells were suspended in 10 mM phosphate buffer (pH 7.5) and then lysed on ice by sonicating twice for 15 s. Triton X-100 (1%) was then added to the lysates and incubated for 10 min on ice. The lysates were clarified, by centrifugation at 5,000xg for 10 min at 4◦C, to remove cellular debris. The protein content of the supernatant was determined by the Bradford method, using bovine serum albumin as the standard. The total SOD activity was used to detect the level of epinephrine auto-oxidation inhibition [29]. Fifty microgram of protein was added to 500 mM phosphate buffer (pH 10.2) and 1mM epinephrine. Epinephrine rapidly undergoes auto-oxidation at pH 10 to produce adrenochrome, a pink-colored product, which was assayed at 480 nm using a UV/VIS spectrophotometer in the kinetic mode. SOD inhibits the auto-oxidation of epinephrine. The rate of inhibition was monitored at 480 nm, and the amount of enzyme required to produce 50% inhibition was defined as one unit of enzyme activity. The total SOD activity was expressed as units per milligram protein.

2.17. Statistical analysis

All the measurements were made in triplicate and all values were represented as means ± standard error (SE).The results were subjected to an analysis of the variance (ANOVA) using the Tukey test to analyze the difference. $P<0.05$ were considered significantly.

3. Results

3.1. The effect of luteolin on ROS scavenging in cell-free system and intracellular system.

The hydroxyl radicals generated by the Fenton reaction ($FeSO_4$+H_2O_2) in a cell-free system was detected by ESR spectrometery. The ESR data revealed that a signal was not observed for the control and luteolin at 2.5 μg/ml, however, the signal of the hydroxyl radical increased up to 2621 in the $FeSO_4$+H_2O_2 system. Pretreatment of luteolin decreased hydroxyl radical signal to 237. (Fig.2A) Superoxide radicals which are generated by Xanthine/xanthine oxidase were detected by ESR spetrometery. As shown Fig.2.B, the signal of the Superoxide radicals increased up to 902 in the Xanthine/xanthine oxidase system. Pretreatment of luteolin decreased superoxide radical signal to 573 (Fig.2B) Intracellular reactive oxygen species (ROS) detected by 2′,7′-dichlorodihydrofluorescein diacetate (DCF-DA) dye. Confocal microscopy revealed that luteolin reduced the red fluorescence intensity with H_2O_2 treatment (Fig. 2C)

A.

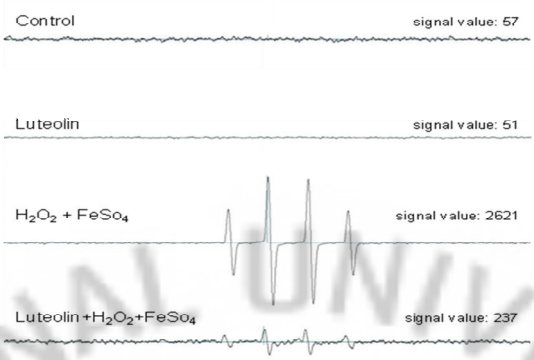

B.

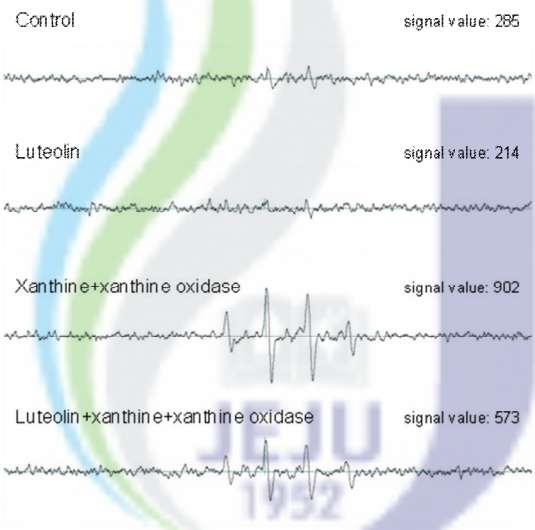

FIG 2. Effect of luteolin on the scavensing of hydroxyl radicals and superoxide radicals and intracellular ROS. (A) Hydroxyl radicals generated by the fenton reaction (H_2O_2+$FeSO_4$) were reacted with DMPO, and the resultant DMPO-OH adducts were detected by ESR spectrometry. (B) Superoxide radicals generated by the xanthine and xanthine oxidase were reacted with DMPO, and the resultant DMPO-OOH adducts were detected by ESR spectrometry.

C.

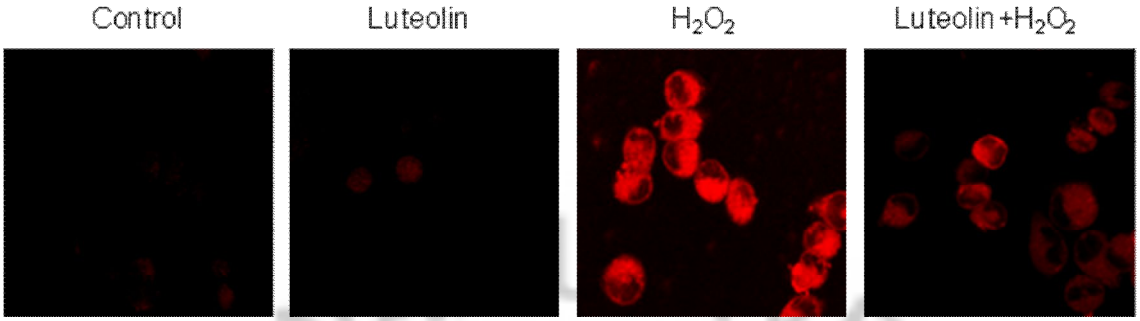

FIG 2. Effect of luteolin on the scavensing of hydroxyl radicals and superoxide radicals and intracellular ROS. (A) Hydroxyl radicals generated by the fenton reaction (H_2O_2+$FeSO_4$) were reacted with DMPO, and the resultant DMPO-OH adducts were detected by ESR spectrometry. (B) Superoxide radicals generated by the xanthine and xanthine oxidase were reacted with DMPO, and the resultant DMPO-OOH adducts were detected by ESR spectrometry. (C) Intracellular ROS was detected by the DCF-DA method.

3.2. The effect of luteolin on H_2O_2-induced lipid peroxidation.

The ability of luteolin to inhibit membrane lipid peroxidation in H_2O_2-treated cells was investigated. Lipid peroxidation was tested by diphenyl-1-pyrenylphosphine. (DPPP) DPPP reacts with lipid hydroperoxides stoichio-metrically to yield highly fluorescent product DPPP oxide [30]. As shown in Fig. 3A, DPPP fluorescent intensity had dramatically increased in hydrogen peroxide treated cells, however, treatment with 2.5 µg/ml luteolin decrease the fluorescent intensity. Moreover, Fig.3B, V79-4 cells exposed to H_2O_2 revealed an increase in lipid peroxidation, which was substantiated by the generation of TBARS. However, luteolin prevented the H_2O_2-induced peroxidation of lipids.

3.3. The effect of luteolin against the damage of DNA

Cellular DNA damage induced by H_2O_2 exposure was detected by an comet assay. Treatment of H_2O_2 was found to increase the tail length and percentage of DNA in the tail to 77%, however, pretreatment with luteolin at 2.5µg/ml decreased the tail length and percentage of DNA in the tail to 51% (Fig. 4B). The phosphorylation of the nuclear histone H2A.X is a sensitive marker for DNA double strand breakage [31]. As shown fig 4C, Pretreatment of luteolin decreased the Phospho H2A.X expression compared with the H_2O_2 treated cell.

A.

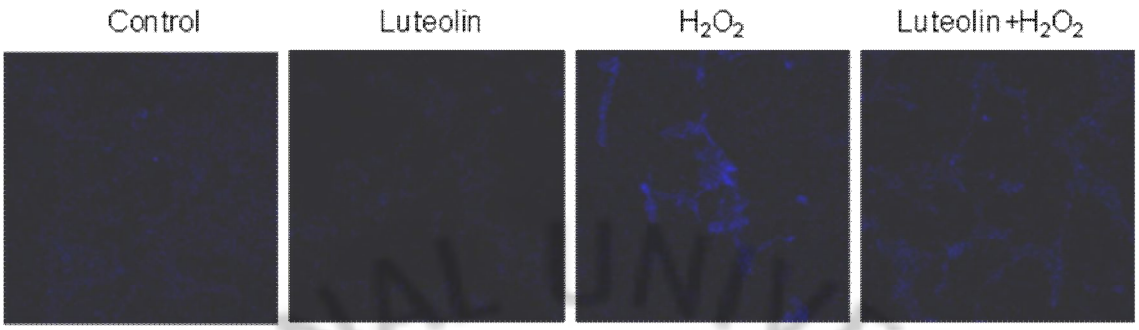

B.

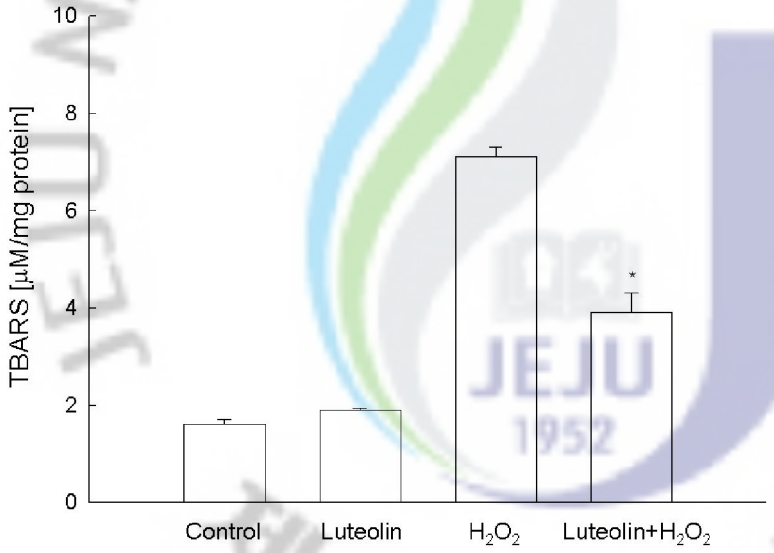

FIG 3. The effect of luteolin on H_2O_2 induced lipid peroxidation. (A) Lipid peroxidation detected by DPPP staining and (B) by measuring the amount of TBARS. *significantly different from H_2O_2 treated cells ($p<0.05$)

A.

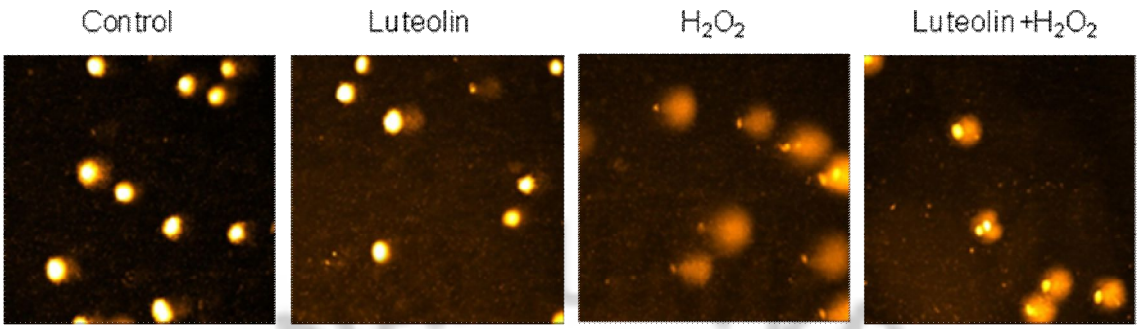

B.

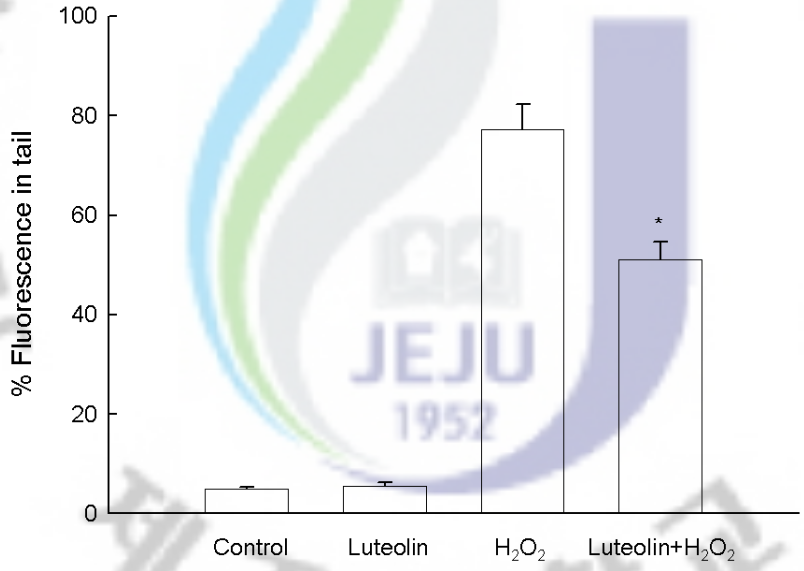

FIG 4. The effect of luteolin on H_2O_2 induced DNA damage. (A) Representative images and (B) percentage of cellular DNA damage were detected by an alkaline comet assay. The measurements were made in triplicate and the values were expressed as means±SE. *significantly different from H_2O_2 treated cells ($p<0.05$)

C.

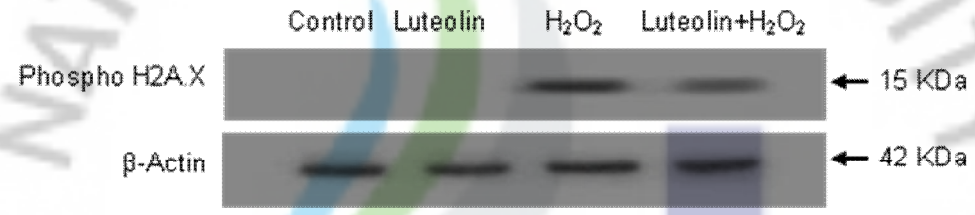

FIG 4. The effect of luteolin on H_2O_2 induced DNA damage. (C) Protein expression of phospho H2A.X was determined by western blot analysis.

3.4. The effect of luteolin on cell survival in H_2O_2

In order to know the effect of the luteolin on cell viability, Cells were treated with luteolin at 2.5 μg/ml for 1 h prior to the addition of H_2O_2. The cell viability was determined 24 h later by the MTT assay. As shown in Fig. 5A, Combination with luteolin at 2.5μg/ml and H_2O_2 increased the cell viability up to 77% compared to 54% in H_2O_2-treated cells. Moreover, to evaluate the cytoprotective effects of luteolin on apoptosis induced by H_2O_2, the nuclei of the V79-4 cells were stained with Hoechst 33342 and assessed by microscopy. As shown Fig. 5B, H_2O_2-treated cells induced the significant nuclear fragmentation, apoptotic morphology. However, when the cells were pretreated with luteolin for 1 h prior to H_2O_2 treatment, a decrease in nuclear fragmentation was observed. As shown in Fig. 5C, H_2O_2-treated cells revealed a 33% increase in the apoptotic sub-G1 DNA content. Moreover, Pretreatment with 2.5 μg/ml of luteolin decreased the apoptotic sub-G1 DNA content to 12%. Next, We examined the Bcl-2 families and caspase 3 (17 kDa) and caspase 9 (37 kDa) protein expression detected by western blot. Fig.5D showed that the Bax, a pro-apoptotic protein, decreased in H_2O_2 treated cells and the Bcl-2, a anti-apoptotic protein, recovered in luteolin and H_2O_2 cells. It was also observed the decreased activation of caspase 3 (17 kDa), caspase 9 (37, 39kDa) in pretreated with luteolin.

A.

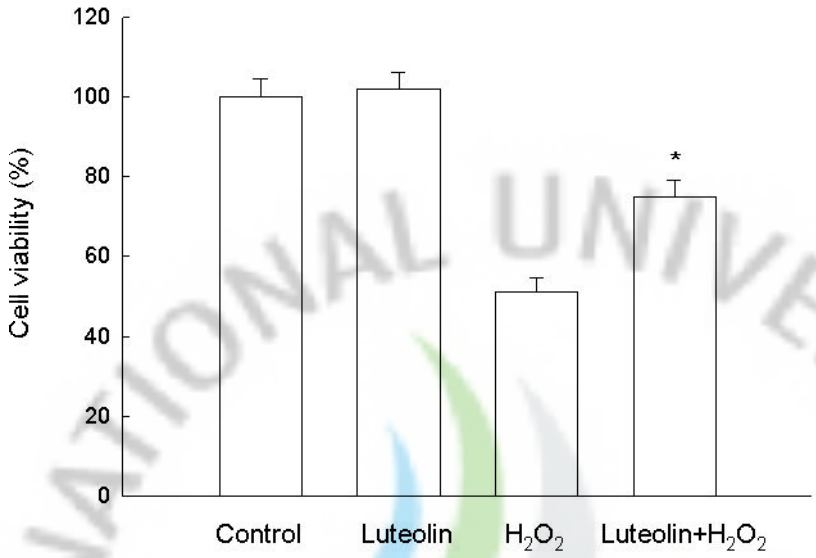

B.

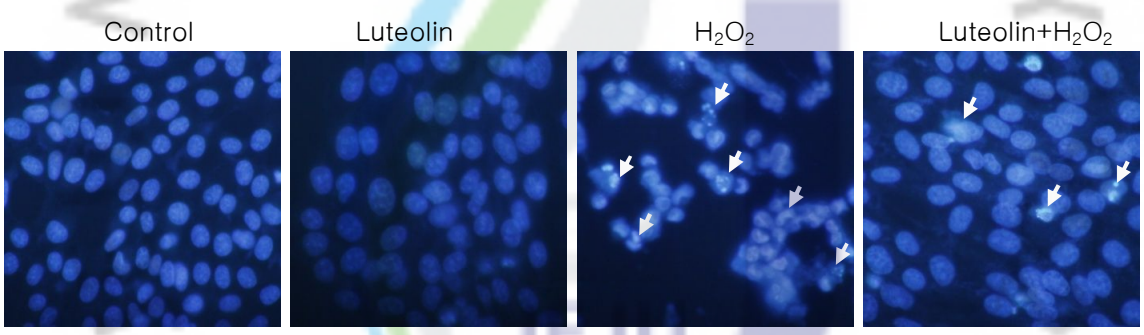

FIG 5. The effect of luteolin on H_2O_2 induced apoptosis. (A) Cell viability was determined by MTT assay. *significantly different from the value of H_2O_2 treated cells ($p<0.05$) (B) Apoptotic body was observed by Hoechst 33342 staining. Apoptotic bodies are indicated by arrows.

C.

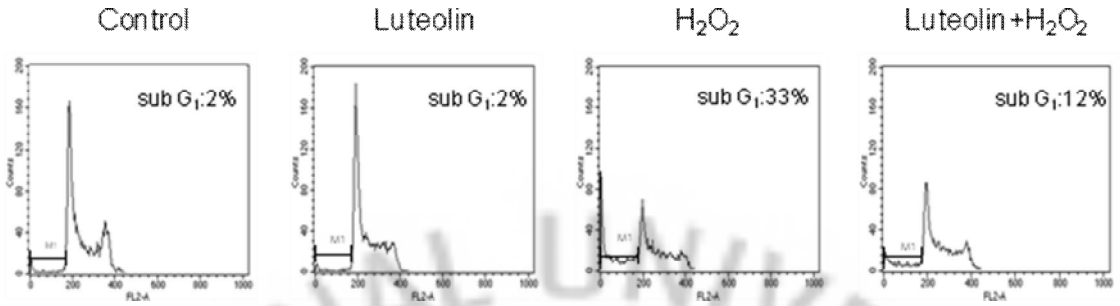

D.

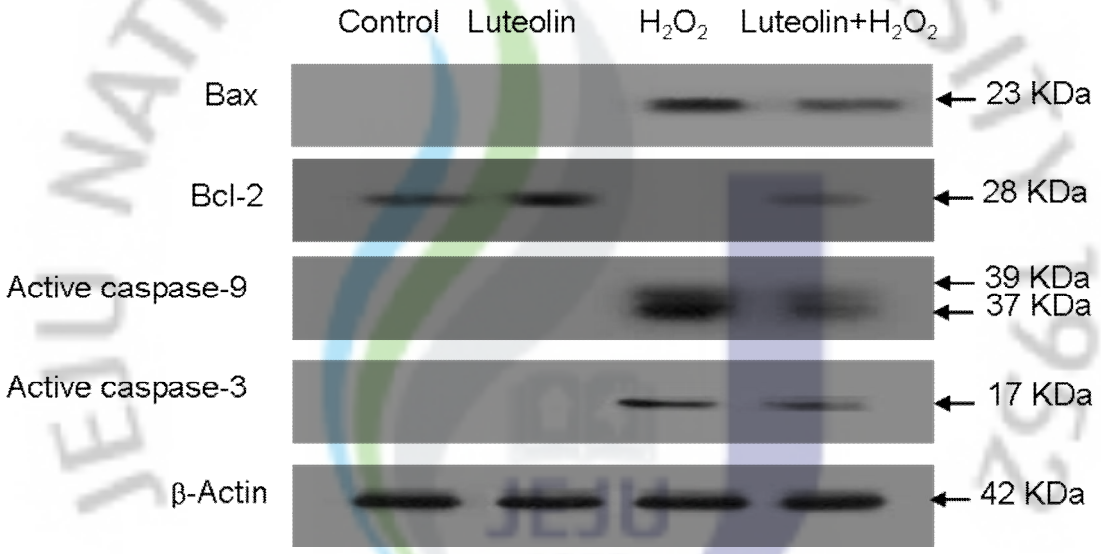

FIG 5. The effect of luteolin on H_2O_2 induced apoptosis. (C) Apoptotic sub G_1 content was detected by flow cytometry. (D) Western blot analysis was performed using anti-Bax, Bcl-2, Caspase-3 and 9 antibodies.

3.5. The effect of luteolin on glutathione(GSH) and γ-GCL

The intracelluar GSH level was determined by using a GSH-sensitive fluorescence dye CMAC. As shown in Fig. 6.A, Pretreated with H_2O_2 cell showed significant reduction of GSH level in confocal data. However, treated with luteolin for 1 h prior to H_2O_2 treatment, a increase in GSH level was observed. To investigate the upstream of GSH, We examined the effect of γ-GCL by western blot. Gamma-glutamylcysteine synthetase (glutamate cysteine ligase, GCL) is the first enzyme in the glutathione biosynthesis. Fig 6.B showed the H_2O_2 treatment cell significantly decrease the γ-GCL protein expression, However, pretreated with luteolin increase the protein expression level.

3.6. The Effect of luteolin on Intracellular Antioxidant enzymes

In order to know the Intracellular Antioxidant enzymes protein expression, western blot analysis was performed. Fig.7A showed that H_2O_2 treated cells decreased the Cu/Zn SOD, CAT, GPx, HO-1 protein expression. However, luteolin restored the protein expression compared with the H_2O_2 treated cells. Moreover, pretreatment of luteolin increased the SOD (28.5 units/mg protein), CAT (17.3 units/mg protein), Gpx (17.3 units/mg protein), HO-1 (16.7 pmol of bilirubin/mg protein/min) enzyme activities compared with H_2O_2 treated SOD (22.5 units/mg

protein), CAT (8.6 units/mg protein), Gpx (8.6 units/mg protein), HO-1 (8.6 pmol of bilirubin/mg protein/min) enzyme activities. (Fig.7B)

A.

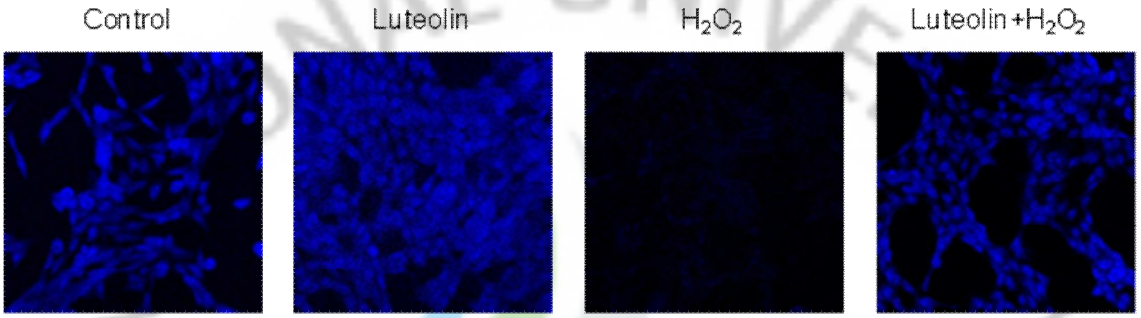

B.

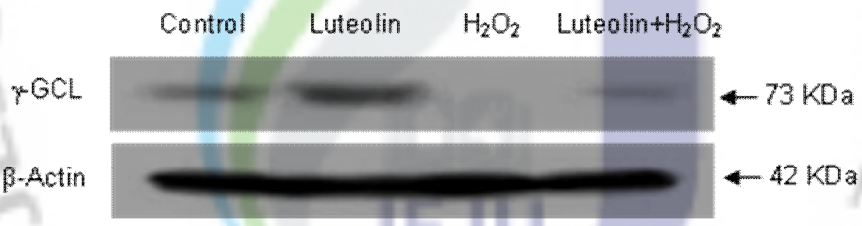

FIG 6. The effect of luteolin on glutathione(GSH) and γ-GCL. (A) Intracelluar GSH level was determined by using CMAC dye. (B) Western blot analysis was performed using anti-γ-GCL antibody.

A.

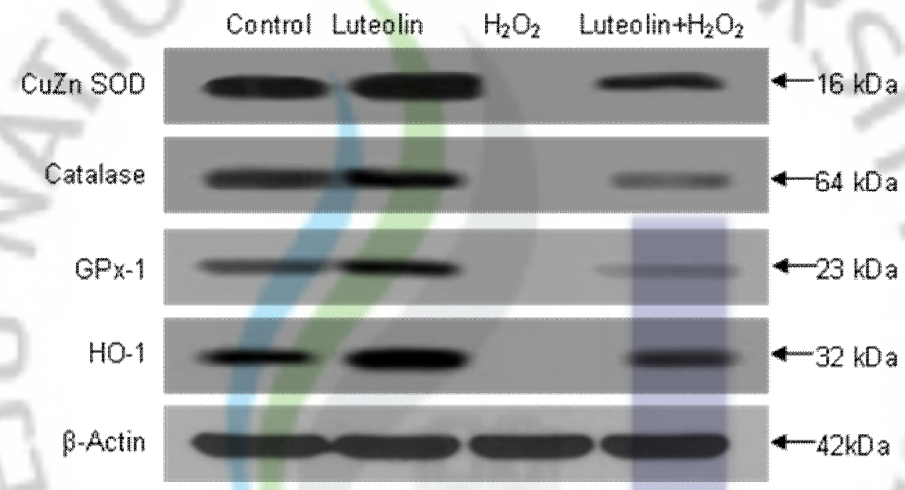

FIG 7. The effect of luteolin on intracellular Antioxidant enzymes. (A) Western blot analysis was performed using Cu/Zn SOD, CAT, Gpx, HO-1 specific antibodies.

B

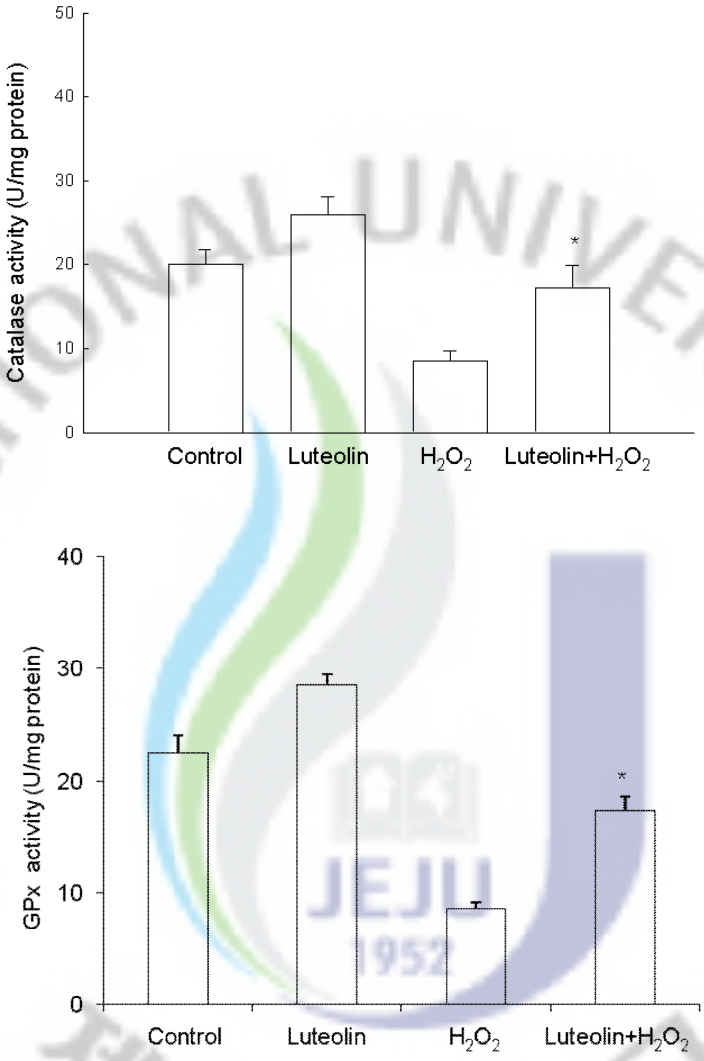

FIG 7. The effect of luteolin on intracellular Antioxidant enzymes. (B) The CAT, SOD, GPx activity is expressed as the average enzyme U/mg protein ± SE. HO-1 activity is expressed as pmole of bilirubin per mg protein ± standard error. Asterisk indicates significant difference from the values of H_2O_2-treated cells. ($p<0.05$)

B

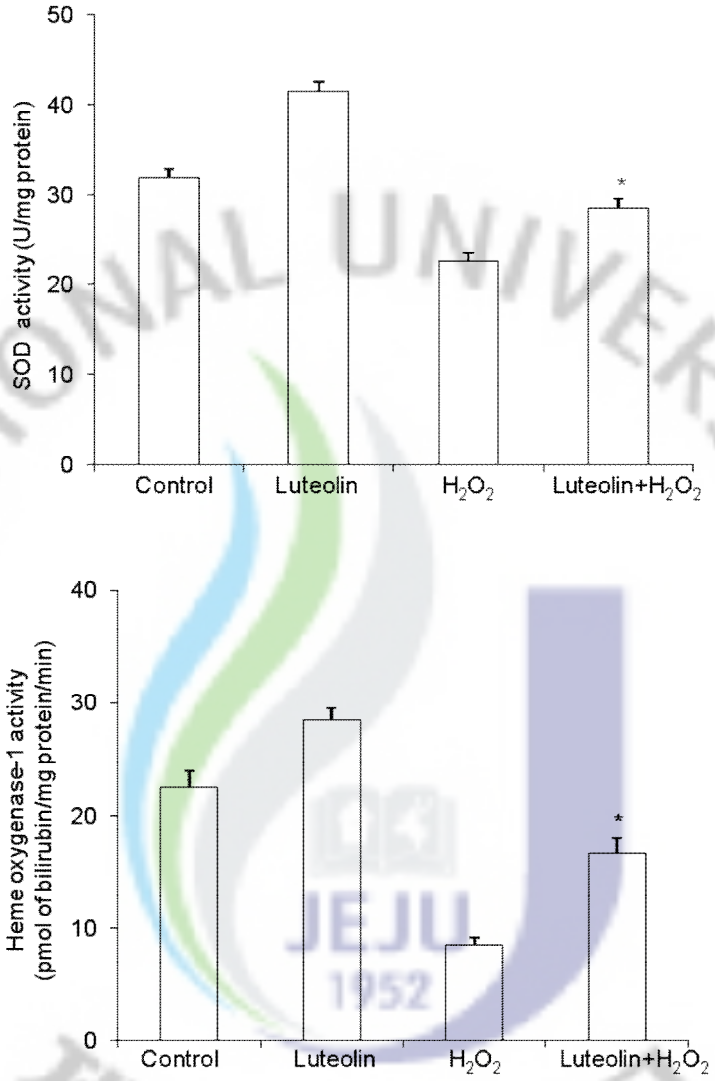

FIG 7. The effect of luteolin on intracellular Antioxidant enzymes. (B) The CAT, SOD, GPx activity is expressed as the average enzyme U/mg protein ± SE. HO-1 activity is expressed as pmole of bilirubin per mg protein ± standard error. Asterisk indicates significant difference from the values of H_2O_2-treated cells. ($p<0.05$)

4.Discussion

Flavonoid has polyphenol groups which are found in coffee, beer, wine and fruits and vegetables. Polyphenols have reported to reduce the risk of cardiovascular disease and cancer [32]. In addition, it has antioxidant capacity in KB cells [33]. Flavonoids also contain the polyphenol groups. For the reason, many researchers have studied on the flavonoid compounds. EGCG (Epigallocatechin gallate) from green tea extract protects the human retinal pigment epithelial cells against the UV irradiation [34] and esculetin inhibit the cell proliferation in human leukemia U937 cells [35]. Flavonoids have reported to exext the antioxidant effect via the antioxidant enzyme activation [36]. Luteolin, one of the flavonoids, has reported the benefit effects in the cells and in vivo [13-16]. Although many studies have reported the antioxidant activity of flavonoids, there is no report on the antioxidant effect of luteolin in lung fibroblast cells. In this study, we investigate the effect of luteolin in lung fibroblast cells. ROS are very small molecules that include oxygen ions and peroxides. ROS can attact to the cell damage and finally cause many diseases [3-7]. H_2O_2 is one of the reactive oxygen species and causes the oxidative damage. In this study, Luteolin scavenged the superoxide anions and hydroxyl radicals in a cell-free system. (Fig 2a,b) Furthermore, pretreatment of luteolin dramatically reduced the intracellular ROS level. (Fig 2c)

ROS attacked the cell membrane then to generate the lipid peroxidation [37]. In our study, H_2O_2 significantly induced the lipid peroxidation in the cofocal date and TBARS formation. (Fig 3a,b), However, Luteolin prevented the cell membrane lipid peroxidation. H_2O_2 can induce cellular DNA damage including DNA base modification and DNA strand breakage [38]. In this study, Treatment of H_2O_2 cells increased the DNA damage and phospho-H2A.X protein, However, pretreatment of luteolin reduced DNA damage as well as the H2A.X protein expression. H_2O_2 can significantly induce the apoptosis, however, luteolin inhibited the apoptosis. Cells treated with H_2O_2 exhibited the cell death, apoptotic bodies, apoptotic sub-G1 DNA contents. (Fig 5a-c) In order to know the mechanisms of apoptosis, we observed the mitochondrial cell death pathway related protein. Mitochondrial cell death pathway is the major target of cell death pathway. In many cells, ROS induced apoptosis through the mitochondrial cell death pathway [39-40]. As shown Fig 5D, Luteolin reduced the levels of the active forms of caspase 9 and 3, reduced the pro-apoptotic protein bax and elevated the anti-apoptotic protein bcl-2. In order to prevent the oxidative damage, cells have antioxidant enzymes. Antioxidant enzymes such as superoxide dismutase (SOD), catalase (CAT), glutathione peroxidase (GPx) and Hemeoxygenase-1 (HO-1) protect the cells against the cellular damage by the ROS [41-44]. In our study, we observed the decreased level of SOD, CAT, Gpx, HO-1, protein expression and

activities in H_2O_2 treated cells and pretreated of luteolin restored the protein expression and activities. (Fig 7) Taken together we have shown that luteolin can inhibit the ROS formation by reducing the cellular damage via the increasing the actioxidant enzyme activities.

5. References

[1] Baran CP, Zeigler MM, Tridandapani S, Marsh CB, The role of ROS and RNS in regulating life and death of blood monocytes. Curr. Pharm. Des 2004;10;855-866.

[2] Park IJ, Hwang JT, Kim YM, Ha JH, Park OJ, Differential Modulation of AMPK Signaling Pathways by Low or High Levels of Exogenous Reactive Oxygen Species in Colon Cancer Cells. Ann. N.Y. Acad. Sci 2006;1091;102-109.

[3] Zhang R, Kang KA, Piao MJ, Ko DO, Wang ZH, Lee IK, Kim BJ, Jeong IY, Shin Tk, Park JW, Lee NH, Hyun JW, Eckol protects V79-4 lung fibroblast cells against γ-ray radiation-induced apoptosis via the scavenging of reactive oxygen species and inhibiting of the c-Jun NH2-terminal kinase pathway. European Journal of Pharmacology 2008;591;114-123.

[4] Rezvani HR, Mazurier F, Andre MC, Pain C, Ged C, Taıeb A, Verneuil HD, Protective Effects of Catalase Overexpression on UVB-induced Apoptosis in Normal Human Keratinocytes. The Journal of biological chemistry 2006;281;17999-18007.

[5] Liu Z, Lu H, Shi H, Du Y, Yu J, Gu S, Chen X, Liu KJ, Hu CA, PUMA Overexpression Induces Reactive Oxygen Species Generation and Proteasome-Mediated Stathmin Degradation in Colorectal Cancer Cells. Cancer Res 2005;65;1647-1654.

[6] Morris PE, Bernard GR, Significance of glutathione in lung disease and implications for

therapy. Am. J. Med. Sci 1994;307;119-127.

[7] Nguyen C, Teo JL, Matsuda A, Eguchi M, Chi EY, Henderson WR, Kahn JM, Chemogenomic identification of Ref-1/AP-1 as a therapeutic target for asthma. Proc. Natl. Acad. Sci. USA 2003;100;1169-1173.

[8] Du D, Chang S, Chen B, Zhou H, Chen ZK, Heme Oxygenase-1 Protects INF−┌ Primed Endothelial Cells From Jurkat T-Cell Adhesion. Transplantation Proceedings 2007;39;3449-3451.

[9] Lee SR, Suk KH, Heme oxygenase-1 mediates cytoprotective effects of immunostimulation in microglia. biochemical pharmacology 2007;74;723-729.

[10] Rice-Evans CA, Miller NJ, Paganga G, Structure-antioxidant activity relationships of flavonoids and phenolic acids. Free Radical Biol. Med 1996;20;933-956.

[11] Wang X, Hao MW, Dong K, Lin F, Ren JH, Zhang HZ, Apoptosis Induction Effects of EGCG in Laryngeal Squamous Cell Carcinoma Cells through Telomerase Repression. Arch Pharm 2009;32;1263-1269.

[12] Shimoi K, Okada H, Furugori M, Goda T, Takase S, Suzuki M, Intestinal absorption of luteolin and luteolin 7-O-beta-glucoside in rats and humans. FEBS Lett 1998;438;220-224.

[13] Cristina PR, Xavier, Cristovao FL, Ana P, Raquel S, Manuel FF, Cristina PW, Luteolin,

quercetin and ursolic acid are potent inhibitors of proliferation and inducers of apoptosis in both KRAS and BRAF mutated human colorectal cancer cells. Cancer Letters 2009;281;162-170.

[14] Shi RX, Ong CN, Shen HM, Luteolin sensitizes tumor necrosis factor-α-induced apoptosis in human tumor cells. Oncogene 2004;23;7712-7721.

[15] Cai Q, Rahn R, Zhanga RW, Dietary flavonoids, quercetin, Luteolin and genistein, reduce oxidative DNA damage and lipid peroxidation and quench free radicals. Cancer Letters 1997;119;99-107.

[16] Sadzuka Y, Sugiyama T, Shimoi K, Kinae N, Hirota S, Protective effect of flavonoids on doxorubicin-induced cardiotoxicity. Toxicology Letters 1997;92;1-7.

[17] Chen HQ, Jin ZY, Wang XJ, Xu XM, Deng L, Zhao JW, Luteolin protects dopaminergic neurons from inflammation-induced injury through inhibition of microglial activation. Neuroscience Letters 2008;448;175-179.

[18] Yoshimura Y, Inomata T, Nakazawa H, Kubo H, Yamaguchi F, Ariga T, Evaluation of free radical scavenging activities of antioxidants with an H_2O_2/NaOH/DMSO system by electron spin resonance. J. Agric. Food Chem 1999;47;4653-4656.

[19] Rimbach G, Weinberg PD, Pascual-Teresa SD, Alonso MG, Ewins B, Turner R, Minihane

AM, Botting N, Firley B, Matsugo S, Uchida Y, Cassidy A, Sulfation of genistein alters its antioxidant properties and its effect on platelet aggregation and monocyte and endothelial function. Biochim. Biophys. Acta 2004;1670;229-237.

[20] Rosenkranz AR, Schmaldienst S, Stuhlmeier KM, Chen W, Knapp W, Zlabinger GJ, A microplate assay for the detection of oxidative products using 2′, 7′-dichlorofluorescein-diacetate. J. Immunol. Meth 1992;156;39-45.

[21] Okimoto Y, Watanabe A, Niki E, Yamashita T, Noguchi N, A novel fluorescent probe diphenyl-1-pyrenylphosphine to follow lipid peroxidation in cell membranes. FEBS Lett 2000;474;137-140.

[22] Ohkawa H, Ohishi N, Yagi K, Assay for lipid peroxides in animal tissues by thiobarbituric acid reaction. Anal. Biochem 1979;95;351-358.

[23] Carmichael J, DeGraff WG, Gazdar AF, Minna JD, Mitchell JB, Evaluation of atetrazolium-based semi automated colorimetric assay: assessment of chemo-sensitivity. Cancer Res 1987;47;936-941.

[24] Nicoletti I, Migliorati G, Pagliacci MC, Grignani F, Riccardi C, A rapid and simple method for measuring thymocyte apoptosis by propidium iodide staining and flow cytometry. J. Immunol. Meth 1991;139;271-279.

[25] Ohkawa H, Ohishi N, Yagi K, Assay for lipid peroxides in animal tissues by thiobarbituric acid reaction. Anal. Biochem 1979;95;351-358.

[26] Paglia DE., Valentine WN, Studies on the quantitative and qualitative characterization of erythrocyte glutathione peroxidase. J. Lab. Clin. Med 1967;70;158-164.

[27] Kutty RK, Maines MO, Oxidation of heme c derivatives by purified heme oxygenase in the rat liver. J. Biol. Chem 1982;257;9944-9952.

[28] Bradford MM, A rapid and sensitive method for the quantitation of microgram quantities of protein utilizing the principle of protein-dye binding. Anal. Biochem 1976;72;248-254.

[29] Misra HP, Fridovich I, The role of superoxide anion in the autoxidation of epinephrine and a simple assay for superoxide dismutase. J Biol Chem 1972;247;3170-3175.

[30] Okimoto Y, Watanabe A, Niki E, Yamashita T, Noguchi N, A novel fluorescent probe diphenyl-1-pyrenylphosphine to follow lipid peroxidation in cell membranes. FEBS Letters 2000;474;137-140.

[31] Rogakou EP, Pilch DR, Orr AH, Ivanova VS, Bonner WM, DNA double-stranded breaks induce histone H2AX phosphorylation on serine 139. J. Biol. Chem 1988;273;5858-5868.

[32] Arts IC, Hollman PC, Polyphenols and disease risk in epidemiologic studies. American Journal Clinical Nutrition 2005;81;317-325.

[33] Mei Y, We D, Liu J, Reversal of Multi drug Resistance in KB Cells with Tea Polyphenol Antioxidant Capacity. 2005;4;468-473.

[34] Yang SW, Lee BR, Koh JW, Protective Effects of EpigallocatechinGallate after UV Irradiation in Cultured Human Retinal Pigment Epithelial Cells. Korean Journal of Ophthalmology 2007;21;232-237.

[35] Lee SH, Park C, Jin CY, Kim GY, Moon SK, Hyun JW, Lee WH, Choi BT, Kwon TK, Yoo YH, Choi YH, Involvement of extracellular signal-related kinase signaling in esculetin induced G_1 arrest of human leukemia U937 cells. Biomedicine & Pharmacotherapy 2008;62;723-729.

[36] Piao MJ, Kang KA, Zhang R, Ko DO, Wang ZH, You HJ, Kim HS, Kim JS, Kang SS, Hyun JW, Hyperoside prevents oxidative damage induced by hydrogen peroxide in lung fibroblast cells via an antioxidant effect. Biochimica et Biophysica Acta 2008;1780;1448-1457.

[37] Denisova NA, Cantuti-Castelvetri I, Hassan WN, Paulson KE, Joseph JA, Role of membrane lipids in regulation of vulnerability to oxidative stress in PC12 cells: implication for aging. Free Radic. Biol. Med 2001;30;671-678.

[38] Zhang R, Kang KA, Piao MJ, Maeng YH, Lee KH, Chang WY, You HJ, Kim JS, Kang SS,

Hyun JW, Cellular protection of morin against the oxidative stress induced by hydrogen peroxide. Chemico-Biological Interactions 2009;177;21-27.

[39] Laethem AV, Nys K, Kelst SV, Claerhout S, Ichijo H, Vandenheede JR, Garmyn M, Agostinis P, Apoptosis signal regulating kinase-1 connects reactive oxygen species to p38 MAPK-induced mitochondrial apoptosis in UVB-irradiated human keratinocytes. Free Radical Biology & Medicine 2006;41;1361-1371.

[40] Figueroa S, Oset-Gasque MJ, Arce C, Martinez-Honduvilla CJ, Gonzalez MP, Mitochondrial Involvement in Nitric Oxide-Induced Cellular Death in Cortical Neurons in Culture. Journal of Neuroscience Research 2006;83;441-449.

[41] Murley JS, Kataoka Y, Weydert CJ, Oberley LW, Grdina DJ, Delayed radioprotection by nuclear transcription factor kappaB-mediated induction of manganese superoxide dismutase in human micro vascular endothelial cells after exposure to the free radical scavenger WR1065. Free Radic Biol Med 2006;40;1004-1016.

[42] Arita Y, Harkness SH, Kazzaz JA, Koo HC, Joseph A, Melendez JA, Davis JM, Chander A, Li Y, Mitochondrial localization of catalase provides optimal protection from H_2O_2-induced cell death in lung epithelial cells. Am J Physiol Lung Cell Mol Physiol 2006;290;978-986.

[43] Prasad NR, Menon VP, Vasudev V, Pugalendi KV, Radioprotective effect of sesamol on γ-radiation induced DNA damage, lipid peroxidation and antioxidants levels in cultured human lymphocytes. Toxicology 2005;209;225-235.

[44] Du D, Chang S, Chen B, Zhou H, Chen ZK, Heme Oxygenase-1 protects IFN– γ primed endothelial cells from jurkat T-Cell adhesion. Transplantation Proceedings 2007;39;3449-3451.

6. Abstract in Korean

이 논문은 H_2O_2로 유도된 산화적 스트레스에 대한 luteolin의 세포보호 효과에 대해 연구 하였다. Lyteolin은 xanthine/xanthine oxidase 와 Fenton 반응을 통해 생성된 superoxide radical과 hydroxyl radical을 cell free system에서 소거함을 나타내었다.

게다가 V79-4 chinese hamster lung fibroblast cell에서 H_2O_2처리시 세포 내 ROS가 상당히 증가함을 확인할 수 있었다. Luteolin처리시 H_2O_2로 유도된 세포 내 ROS와 cellular components인 lipid와 DNA손상을 줄임을 확인하였다.

Luteolin처리시 세포 생존률을 증가시켰으며, H_2O_2로 유도된 apoptosis를 mitochondria mediated caspases pathway를 통해 억제함을 나타내었다. Luteolin은 active caspase 3, 9 그리고 Bax의 발현을 줄였고, bcl-2의 발현을 증가시켰다.

게다가 Luteolin은 환원형 글루타치온 reduced glutathione (GSH) level을 회복시켰으며, GSH합성에 관여하는 효소인 glutamate-cysteine ligase (GCL) 발현도 증가시켰다.

게다가 Luteolin은 세포 내 항산화 효소인 superoxide dismutase (SOD), catalase (CAT), glutathione peroxidase (GPx) and hemeoxygenase-1 (HO-1) 활성과 발현을 증가시켰다.

따라서 이 논문에서 Luteolin은 ROS소거와 항산화 효소의 활성을 통해 H_2O_2로 유도된 세포손상을 보호함을 나타내었다.

7 감사의 글

지난 2년 동안 대학원 생활을 하면서 많은 것을 배웠습니다. 대학원 생활 동안 많은 분들의 도움으로 저의 부족한 부분을 채워 나갈 수 있었습니다.

아직도 많은 부분에서 부족함을 느끼고 있기 때문에 더욱더 발전해 나가는 모습을 보여야겠다고 생각 듭니다.

먼저 부족한 저에게 격려와 애정을 아끼지 않고 지도해주신 현진원 교수님께 진심으로 감사 드립니다.

그리고 논문의 부족한 점을 점검해주신 고영상 교수님, 강희경 교수님과 여러 교수님께도 감사의 말씀 올립니다.

실험실의 경아 누나, 미경 누나, 장예, 기천 그리고 지금은 중국에 가있는 지홍이 실험실 생활하면서 저를 많이 도와 주었습니다. 감사합니다.

앞으로 나날이 발전 하기를 바랍니다. 그리고 타 실험실에 있는 선배님과 후배들 역시 감사합니다. 항상 행운이 따르길 바랍니다.

마지막으로 격려와 응원을 보내준 친구들, 부모님께도 감사하다는 말씀을 전합니다. 열심히 하겠습니다. 감사합니다.